Automated AutoCAD Drawing Assessment via Image Processing and Vector Transformation Techniques

Zhengkai Xiong, Jiaming Ge, Rong Wei*
Department of Mechanical and Electrical Engineering, Cangzhou Technical College, Cangzhou City, Hebei Province, 061000, China
E-mail: xzk870036@163.com, JiamingGe68@163.com, weirong525@163.com
*Corresponding author

Keywords: graphics processing, computer graphics. information extraction, computer graphics examination system, computer-aided design (CAD)

Received: April 28, 2025

Conventional assessment practices in computer graphics courses, particularly those that utilize AutoCAD, often rely on manual grading or basic template-matching strategies. These methods are ineffective and biased, particularly when used for extensive evaluations. Intelligent evaluation methods and automated image processing must be integrated as educational technology continues to evolve. The purpose of the proposed effort is to develop and put into use an intelligent AutoCAD computer drawing evaluation system that uses image processing technologies. Enhancing assessment accuracy, automating scoring, and utilizing robotic technologies to combine virtual drawing analysis and actual drawing validation are the objectives. The system evaluates student drawings using MATLAB-based techniques, including vector transformation, grayscale conversion, binarization, and histogram similarity. It extracts components using DXF file parsing, performs geometric matching, and features extraction. A feedback-driven retransmission method ensures packet correctness. A servo motor-powered drawing computer duplicates input drawings, and performance is assessed using torque analysis, picture entropy, consistency, and smoothness criteria. The system could accurately reproduce student drawings with an accuracy of more than 0.1 cm and an average drawing speed of 1.75 cm/s. The system's dependability was confirmed when evaluation ratings for example drawings nearly matched hand grading. Within the robotic arm's torque limits, moment and motion analysis verified operational safety and accuracy. The proposed approach automates computer graphics analysis by combining hardware and software elements for perceptive evaluation. However, limitations on robot motion and image quality sensitivity were limitations, requiring future improvements.

Povzetek: Predstavljen je inteligentni sistem za avtomatsko ocenjevanje risb AutoCAD z obdelavo slik in vektorsko transformacijo. Uporablja DXF analizo, primerjavo slik in robotsko reprodukcijo za natančno in objektivno ocenjevanje.

1 Introduction

Recent advancements in generative models in language and imaging have transformed the perception of computers as co-creators, enabling creative AI to actively participate in idea exploration [1]. Augmented Reality (AR) enhances learning in graphic design education by providing dynamic, 3D-registered visuals, improving students' practical interaction with intricate mechanical structures and spatial comprehension [2]. AutoCAD is a popular program for creating technical drawings and documentation in design and architecture, but beginners may face challenges due to standardized teaching strategies [3].

Automatic List Processing (AutoLISP), a key component of AutoCAD, is a software development tool that automates various engineering and design processes, despite its high skill and work requirements [4]. Screencasts enhance concurrent learning in CAD-based and technical drawing classes, providing flexible, self-paced learning options for students lacking prior CAD experience and limited curriculum time [5]. Conventional CAD systems enhance manufacturing productivity in industries like metallurgy, glass working, and woodturning by facilitating detailed 3D modeling and group technology for small-batch production [6].

The goal of the research is to create and put into use an intelligent AutoCAD computer drawing evaluation system that uses image processing technologies. Enhancing assessment accuracy, automating scoring, and utilizing robotic technologies to combine virtual drawing analysis and actual drawing validation are the objectives.

- To create an automatic AutoCAD assessment system that combines image processing methods with DXF file structure parsing for precise and impartial grading.
- To use sophisticated vector transformation techniques, like skeleton extraction, binarization, and grayscale conversion, to transform visual drawing inputs into formats that could be analyzed.
- To put into practice a feedback-driven retransmission algorithm that replicates annealing principles for effective drawing packet delivery and correction.
- To create a robotic drawing platform with servo motors that could physically replicate digital inputs, confirming the accuracy of vector interpretations.
- To test mechanical drawing precision and compare automated scores with manual grading to assess the accuracy and dependability of the suggested solution.

System organization: Related research on AutoCAD assessment is reviewed in Section 2. The image processing methods, methodology, and DXF file analysis are explained in Sections 3–5. Results, experiments, and system implementation are presented in Sections 6–11. The investigation is concluded in Section 12, which also suggests potential enhancements for evaluation accuracy and scalability.

2 Related work

Employing task performance metrics and rubric-based imagination evaluation with undergraduate students compare the AutoCAD 2025 and AutoCAD Mechanical 2025 CAD tasks' efficiency and creativity. Efficiency and creativity were increased by AutoCAD Mechanical; however, short-term evaluation, a single discipline focus, and a lack of user input analysis cloud were some of the drawbacks [7]. Create an automated evaluation tool for CAD models in mechanical courses that uses a model-based methodology to assess parametric, feature-based, and geometric aspects with parameterization. Although the CAD Model Automatic Assessment (MAA) Tool efficiently automates model evaluation, limitations include restricted validation across several CAD platforms and reliance on teacher-defined coefficients [8]. Sulfur Hexafluoride (SF6) dial pointer recognition system that is accurate and effective, utilizing Computer Aided eXtended Application (CAXA) secondary development for automated CAD drawing generation, open-source computer vision library (OpenCV)-based angle detection, and socket communication. The method achieved a 0.69° average error, exceeding accuracy requirements; restrictions include dependence on particular applications and restricted adaptability to varying dial designs [9]. Following an experiment with focus groups, a literature-informed questionnaire was given to 59 students and 21 educators to assess preferences between hand drafting and CAD in architectural working drawings. CAD was selected for effectiveness and accuracy; restrictions include interest dependence on duplicate instructions and restricted understanding of context during site visits [10]. To enhance the teaching of cosmetics design by incorporating graphic design software, evaluating efficacy, paintbrush choice, and digital design efficiency through comparative tests, two-stage questionnaires, and expert assessments. Computer drawing reduced design time in half and increased the efficacy of instruction; however, the method had drawbacks, such as a learning curve at first and a dependence on particular software capabilities like symmetry functions [11]. Simple brush painting that is automated and realistic. The approach, which was evaluated on the FaceX dataset using Python and TensorFlow, merges an attention mechanism (AM) with a Long Short-Term Memory (LSTM) network. The model's accuracy was 98.63% and the F1 score was 98.75%; however, that requires a lot of processing power and the outcome could differ depending on the dataset [12]. The computer vision system uses wavelet denoising, multi-feature fusion, transfer of style enhancement, and recognition models trained on WikiArt and OilPainting datasets to classify painting styles and analyze sentiment. The model attained 90% sentiment accuracy and over 95% style classification; however, performance could differ when applied to less structured, real-world artwork that wasn't part of benchmark datasets [13]. Table 1 provides the related works summary table.

Table 1: Comparative Summary of the related works

Reference	Method	Dataset	Result	Limitation
Gutiérrez et al. [7]	Comparison of AutoCAD 2025 vs. AutoCAD Mechanical 2025 using performance metrics and creativity rubrics	Undergraduate mechanical engineering students	AutoCAD Mechanical improved efficiency and creativity	Short-term study, single-discipline focus, no user feedback
Eltaief et al. [8]	CAD Model Automatic Assessment (MAA) Tool using parametric,	Mechanical CAD models in an academic setting	Efficient automation of model evaluation	Limited cross-platform validation, depends on teacher-set parameters

	geometric, and feature-based evaluation			
Zhang et al. [9]	SF6 dial pointer recognition using OpenCV, CAXA, and socket communication	Dial images with angle readings	0.69° average error, high precision	Limited generalizability, depends on specific software
Fakhry et al. [10]	Survey with 59 students and 21 educators comparing CAD vs. hand drafting	Architecture coursework and field visits	CAD preferred for accuracy and efficiency	Risk of overusing copy-paste, lack of site context integration
Hsu et al. [11]	Integration of graphic design software in makeup design teaching via experiments and questionnaires	Cosmetology students and experts	Halved design time, improved instructional effectiveness	Initial learning curve, software-dependent (e.g., mirror function)
Zhang [12]	LSTM and attention-based model for automated brush painting (Python + TensorFlow)	FaceX dataset	98.63% accuracy, 98.75% F1 score	High processing cost, dataset-sensitive
Cheng et al. [13]	Computer vision using wavelet denoising, feature fusion, and style transfer	WikiArt and OilPainting datasets	95%+ style classification, 90% sentiment accuracy	Reduced accuracy on non-benchmark, real-world art

Research fills a critical gap by focusing on the absence of intelligent, automatic assessment systems for AutoCAD-based drawings in educational settings. Research combines image processing and vector transformation techniques to provide accurate, objective, and scalable assessment, whereas existing solutions concentrate on manual review or limited automation. The research helps to modernize CAD education, lessen the workload of instructors, and improve the learning experience for students with limited CAD competency by bringing automated outcomes into line with human grading standards and increasing the efficiency of drawing interpretation.

3 Image processing applied to computer graphics examination-related technologies

The use of MATLAB for graphics processing is because MATLAB has strong matrix operation capabilities, so the processed graphics are represented in the form of matrices or vectors [14-15].

Funded by: Daqing Normal University Youth Fund Research Project (No.: 9ZQ08; Teaching Research Project of Heilongjiang Bayi Agricultural University (Project Title: Research and Application of Paperless Exam System in Computer Graphics Courses. The images produced by the differences are similar) The measure of the degree, the normalization can be well realized by using the histogram, the calculation amount is small, the operation speed is fast, and it is the most used method now in calculate the Equation (1).

$$Sim(G,S) = \frac{1}{N}\sum_{i=1}^{N}\left(1 - \frac{|g_i - s_i|}{Max(g_i, s_i)}\right) \quad (1)$$

Here, G and S are the histograms of the target image and the source image$N$ is the amount of color space models, is the image attribute of the block area of the target image, and is the image attribute of the block area of the source image. $g_i\ s_i$

The histogram-based method was chosen. After all, it is more appropriate for real-time AutoCAD examination systems because it is faster to execute and has less processing complexity while keeping competitive accuracy. The applicability of techniques like SSIM and cosine similarity in time-sensitive evaluation environments was diminished by the reality that they only slightly increased accuracy but arrived with much longer processing times.

4 Image acquisition and processing

The typical AutoCAD computer drawing examination system design mathematical model can be expressed by Equation (2), and the calculation of the optimal computer processing analysis $P = \{u_1, u_2, \cdots, u_k\}$:

$$min\, Z\,(P_\alpha) = \sum_{i=1}^{k=1} d\left(u_{\alpha_i}, u_{\alpha_{i+1}}\right) + d\left(u_{\alpha_1}, u_k\right) \quad (2)$$

In the formula, α_i is used to describe the reorganization of the K computer-processed analysis point order and $d\left(u_{\alpha_i}, u_{\alpha_{i+1}}\right)$ describes the Manhattan distance between two points.

The path optimization model for examining AutoCAD drawing elements during assessment is represented by equation (2). Practically speaking, each point u_i represents a feature or object like a wall, door, or window that was taken from a student's artwork and represented as spatial coordinates or data blocks. The function $d\left(u_{\alpha_i}, u_{\alpha_{i+1}}\right)$computes the distance in meters between consecutive features, a pertinent metric in CAD since objects are frequently aligned to orthogonal grids. The variable α_i indicates a sequence of such features as identified by the system. Finding the most effective structural match between the student's layout and the reference drawing is part of minimizing the sum of these distances.

The formula above quantifies the spatial deviation, for instance, if the student's layout rearranges or misaligns the four rooms that are connected linearly in the correct drawing. That allows the system to assess not only the elements' existence but also their arrangement in a sequence that makes sense geometrically and conceptually. The following is the specific discriminant in Equation (3). $d(i,j,u)$: Inputs parameters function.

$$d(i,j,u) = \begin{cases} [0,0,0], if\ \ i \geq a\ and\ j \geq a\ and\ u \geq a \\ [i,j,u], if\ \ i < a\ and\ j < a\ and\ u < a \\ [i,j,u], if\ \ i > b\ and\ j > b\ and\ u > b \end{cases} \quad (3)$$

The corresponding drawing processing drawing information feature vector χ_i The expression in Equation (4).

$$l_\varepsilon(g) = (1-\rho) l_\varepsilon(g-1) + \gamma f\left(\chi_i(g)\right) \quad (4)$$

f : Represents the adaptive function corresponding to the feature drawing feature vector χ_i of the drawing process. $\gamma\chi_i(g)$: The corresponding drawing processing analysis of the εth dispensation in the actual application process. Equation (5) contains for processing π_p in Drawing ProcessingII.

$$Acu\left(\pi_p\right) = NMI\left(\pi_p, \pi^*\right) \quad (5)$$

π_p and π_q represent the processing of drawing processing. If less information is shared with the drawing processing base drawing, the base drawing is less accurate. Drawings based on image processing techniques that define the thorough analysis in terms of accuracy and diversity typical illustration based on an image processing technique include [16-17] in Equation (6).

$$Eval\left(\pi_p\right) = \lambda Acu\left(\pi_p\right) + (1-\lambda) Div\left(\pi_p\right) \quad (6)$$

$\lambda \in [0,1]$: The exactness and variety of drawings handed out are the degree of importance in the complete analysis criteria. Equation (6) uses the diversity $pro\left(\pi_p\right)$ of the image processing method's basic processing in Equation (7) to get the probability $Div\left(\pi_p\right)$ of choosing every drawing processing basic analyzing technique as the evaluation's basic processing

$$pro\left(\pi_p\right) = \frac{Div(\pi_p)}{\sum_{p=1}^{B} Div(\pi_p)} \quad (7)$$

to restore the drawing's natural color and recognition, the drawing processing network module works to optimize each reconstructed drawing's color and spatial placement [18–19]. The formula defines the drawing processing network module's loss function Lip. The following processing losses are displayed: unmasked regions, masked regions $L_{style}^1 + L_{style}^2$: Style loss, anti-loss L_{total}^{inp} : Total difference loss, andL_{per} : Perceptual loss in Equation (8).

$$L_{total}^{inp} = 2L_{valid} + 12L_{hole} + 0.04L_{per} + 100\left(L_{style}^1 + L_{style}^2\right) + 100L_{adv} + 0.3L_{var} \quad (8)$$

L: Loss function. The weight of each loss term in Manhattan distance (MD) is determined by examining 50 tests. The actual and unmasked processing modes are used, with M representing the irregular binary mask, I_{dam} representing the damaged mode, and I_{inp} representing the outcome mode in Equation (9-10).

$$L_{valid} = \left\| M \times \left(I_{inp} - I_{dam}\right) \right\|_1 \quad (9)$$

$$L_{hole} = \left\| (1-M) \times \left(I_{inp} - I_{dam}\right) \right\|_1 \quad (10)$$

Rotate and restore the identification points against the original image. h Is the connection point of the opening draw, placed in the drawing parallel to the identification graph $0 \leq k \leq h\left(vx'_{2k+1,i}, vy'_{2k+1,i}\right)$ for each identification point the following rotation operation is performed in Equation (11)

$$\begin{cases} dx'_k = vx'_{2k+1,i} - vx_{k,i} \\ dy'_k = vy'_{2k+1,i} - vy_{k,i} \end{cases} \begin{bmatrix} vx'_{2k+1,i} \\ vy'_{2k+1,i} \end{bmatrix} = \begin{bmatrix} vx_{k,i} \\ vy_{k,i} \end{bmatrix} + \begin{bmatrix} cos(-\theta) & -sin(-\theta) \\ sin(-\theta) & cos(-\theta) \end{bmatrix} \times \begin{bmatrix} dx'_k \\ dy'_k \end{bmatrix} \quad (11)$$

For each drawing P_i and $\tilde{P}_i$, calculate its barycentric coordinates after removing the last point. In the formula, h is the length (number of nodes) of the i-th graph after the original graph is split, h'_i is inserted into the length that has been found, and Equation (12–13) computes the next two offset values.

$$\begin{cases} \overline{vx'_i} = \frac{1}{h'_i-1}\sum_{k=1}^{h'_i-1} vx'_k \\ \overline{vy'_i} = \frac{1}{h'_i-1}\sum_{k=1}^{h'_i-1} vy'_k \end{cases} \begin{cases} \overline{vx_i} = \frac{1}{h_i-1}\sum_{k=1}^{h_i-1} vx_k \\ \overline{vy_i} = \frac{1}{h_i-1}\sum_{k=1}^{h_i-1} vy_k \end{cases} \quad (12)$$

$$\begin{cases} \Delta x_i = \frac{1}{2h_i-2}\sum_{k=1}^{h_i-1}(vx_{k+1} - vx_k)p_k \\ \Delta y_i = \frac{1}{2h_i-2}\sum_{k=1}^{h_i-1}(vy_{k+1} - vy_k)p_k \end{cases} \quad (13)$$

Anzhao Equations (13-17) respectively compute the recognition points of the perpendicular and parallel organized of each drawing.

①$\Delta x_i \neq 0 \&\& \Delta y_i \neq 0$

$$\begin{cases} qx_j = \sum_{\{i|\frac{i}{c}=j\}} \frac{\overline{vx'_i} - \overline{vx_i}}{\Delta x_i} = \sum_{\{i|\frac{i}{c}=j\}} \tilde{b}_i\alpha = c\tilde{b}_j \circ \alpha \\ qy_j = \sum_{\{i|\frac{i}{c}=j\}} \frac{\overline{vy'_i} - \overline{vy_i}}{\Delta y_i} = \sum_{\{i|\frac{i}{c}=j\}} \tilde{b}_i\alpha = c\tilde{b}_j \circ \alpha \end{cases} \quad (14)$$

②$\Delta x_i = 0$, $\Delta y_i \neq 0$

$$\begin{cases} qx_j = \sum_{\{i|\frac{i}{c}=j\}} \sum_{k=1}^{h_i-2} \frac{\overline{vx_{k,i}} - vx_{k,i}}{(vx_{k+1,i} - vx_{k,i})p_k} = \sum_{\{i|\frac{i}{c}=j\}} \tilde{b}_i\alpha = c\tilde{b}_j\alpha \\ qy_j = \sum_{\{i|\frac{i}{c}=j\}} \frac{\overline{vy'_i} - \overline{vy_i}}{\Delta y_i} = \sum_{\{i|\frac{i}{c}=j\}} \tilde{b}_i\alpha = c\tilde{b}_j\alpha \end{cases} \quad (15)$$

③$\Delta x_i \neq 0, \Delta y_i = 0$

$$\begin{cases} qx_j = \sum_{\{i|\frac{i}{c}=j\}} \frac{\overline{vx'_i} - \overline{vx_i}}{\Delta x_i} = \sum_{\{i|\frac{i}{c}=j\}} \tilde{b}_i\alpha = c\tilde{b}_j\alpha \\ qy_j = \sum_{\{i|\frac{i}{c}=j\}} \sum_{k=1}^{h_i-2} \frac{\overline{vy_{k,i}} - vy_{k,i}}{(vy_{k+1,i} - vy_{k,i}) \circ p_k} = \sum_{\{i|\frac{i}{c}=j\}} \tilde{b}_i\alpha = c\tilde{b}_j\alpha \end{cases} \quad (16)$$

④$\Delta x_i = 0$,$\Delta y_i = 0$

$$\begin{cases} qx_j = \sum_{\{i|\frac{i}{c}=j\}} \sum_{k=1}^{h_i-2} \frac{\overline{vx_{k,i}} - vx_{k,i}}{(vx_{k+1,i} - vx_{k,i})p_k} = \sum_{\{i|\frac{i}{c}=j\}} \tilde{b}_i\alpha = c\tilde{b}_j\alpha \\ qy_j = \sum_{\{i|\frac{i}{c}=j\}} \sum_{k=1}^{h_i-2} \frac{\overline{vy_{k,i}} - vy_{k,i}}{(vy_{k+1,i} - vy_{k,i}) \circ p_k} = \sum_{\{i|\frac{i}{c}=j\}} \tilde{b}_i\alpha = c\tilde{b}_j\alpha \end{cases} \quad (17)$$

Aggregated gradients qx_j, qy_j for group j are defined by equations (14)–(17) based on value changes and spacing$(\Delta x_i, \Delta y_i)$. Weighted by coefficients α and transformation parameter $\tilde{b}_i$, gradients are calculated using either straight finite differences or multistep approximations, depending on whether x/y differences are zero. Calculate numeric information values for each plot in Equation (18).

$$\tilde{m}_j = \begin{cases} 1, \frac{qx_j + qy_j}{2} > 1 \\ 0, \frac{qx_j + qy_j}{2} < 1 \end{cases} \quad (18)$$

Once the digital data has been extracted, verify that the identification is valid. The method recognizes similarities between the unique recognition and the extracted acceptance by using the correlation coefficient $cor(m, \tilde{m})$in Equation (19).

$$cor(m, \tilde{m}) = \frac{\sum_{i=0}^{n-1}(m_i\tilde{m}_i)}{\sqrt{\sum_{i=0}^{n-1} m_i^2}\sqrt{\sum_{i=0}^{n-1} \tilde{m}_i^2}} \quad (19)$$

The digital information $\tilde{m}$ is taken from the recognized graphics, and the correlation coefficient between the digital data m and m is$cor(m, \tilde{m})$.

5 DXF file format

DXF is a data interchange file. AutoCAD supports saving and reading of DXF format files to exchange data with other applications. The DXF file is an ASCII file, so it is helpful to use it as the evaluation basis for the answer, check the correctness and rationality of the software production, and design appropriate scoring rules [20-21]. The proposed AutoCAD test system incorporates image-based similarity scoring with rule-based methods like vector comparisons and DXF parameter matching, ensuring both structural and visual accuracy in assessment, aligning with human evaluation standards, and ensuring a comprehensive evaluation process.

The DXF file consists of six parts: HEADER, CLASSES, TABLES, BLOCKS, ENTITIES, and OBJECTS. Each segment starts with group 0-SECTION and ends with group 0-ENDSEC. The format used here is FORTRAN I3, and the next line of different integer values represents different parameter values, such as strings, integer values, real numbers, etc., which have different meanings.

The DXF parsing method compares graphic primitives based on spatial coordinates from entity definitions. The alignment between student and reference drawings is evaluated using coordinate-based geometric matching. A tolerance criterion accounts for small inconsistencies. Only relevant geometric aspects are highlighted by filtering layer and annotation data.

The system manages multiple DXF layers by parsing each layer separately and comparing those using specific drawing components. DXF entity attributes interpret line styles, allowing for small variations. DXF text entities extract annotations, including text and dimensions, and assess alignment consistency, position, and content about the standard drawing.

Geometric matching of drawing elements and DXF file parsing are the primary methods used for scoring, while image features help confirm the correctness of robotic reproduction.

6 Examination system processing flow

When candidates open the examination questions, they are automatically loaded into the examination system through the interface of VBA and AutoCAD. After the examinee completes the answer, the submit action is executed, and the automatic evaluation engine is started. The software runs in the background, firstly outputs the candidates' answers to the DXF file, detects the corresponding standard answer DXF file according to the test question number, compares, and calculates the score according to the scoring parameter table of the test question package. Then upload it to the server and record it. The design process of the computer drawing test system is displayed in Figure 1.

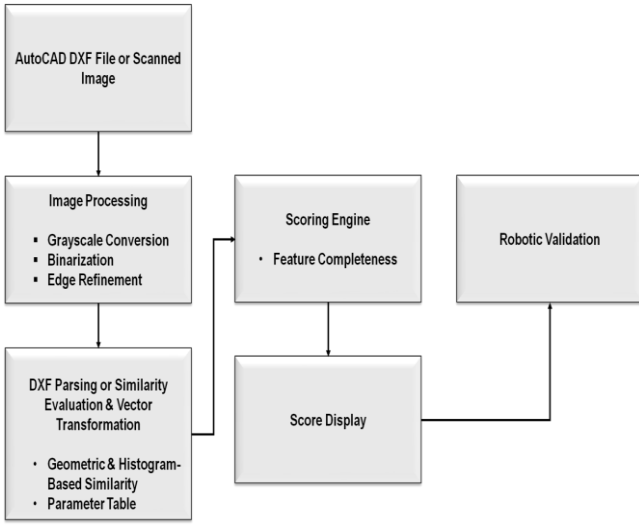

Figure 1: Processing flow of computer graphics examination system.

7 Development tool selection

Because the system is built in AutoCAD, it is executed in AutoCAD, the commonly used software is Visual LISP, VisualC, VisualB a total of three kinds [22], Table 2 is a comparison of the above three kinds of software.

Table 2: Feature comparison of three programming languages.

	flexibility	Easy to learn and use	confidentiality	running speed
Visual C	good	Difference	good	quick
Visual LISP	Difference	good	Difference	slow
Visual B	good	good	good	quick

As can be seen from Table 2, the Visual LISP language is easy to learn but lacks flexibility when completing complex system software. Visual C has strong functions and high flexibility, but it is relatively complex, and programmers have high requirements for computer knowledge, making it difficult to use and grasp quickly. Visual B has the advantages of both Visual LISP and Visual C.

Disadvantage, this is one of the reasons for AutoCAD to switch to Visual B support. Therefore, to develop this system, it is appropriate to use Visual B.

AutoCAD has built-in VBA comprehensive development tools. (VisualBasicforApplication).

8 Design process of computer graphics examination system

Compile the source program with GCC. The driver of the camera is uvcvideo, which supports two formats, YUYV and MPJEG. The device supports the image file imagebmp.bmp captured by the USB camera, such as streaming I/O operations.

Use the ARM-Xilinx-Lnux cross-compilation environment to cross-compile the source files, and copy the executable files generated by compilation to SD. Use the command ARM-Xilinx-Linux-gnuueab-gccv4l2 grab. Compile the c-ozed-camera program, copy the compiled executable file zeed-camera to the Zed-board, connect the USB camera to the Zedboard, connect the cd to the /dev folder, and use the ls command to confirm whether the dev directory is There are videoO devices. Executable files, if

any. Before executing the file, command chmod+x zed-camera or chmod777zed-camera to obtain the executable permission of the file. The former is only valid for the current user; the latter is valid for all users. Execute the executable program according to the command zed-camera, and as shown in Figure 2, code 1 shows the HyperTerminal code.

Code 1: Information is displayed on the HyperTerminal.

Support format:

1. YUV 4: 2: 2($YUYV$)

2. $MJPEG$

$fmt.type$: 1

$pix.pixelformat$: $YUYV$

$pix.height$: 480

$pix.width$: 640

$pix.field$: 1

$init/dev/video0$ [OK]

$grab\ yuyv\ OK$

$save/usr/image\_yuv.yuv\ OK$

$change\ to\ RGB\ OK$

$save/usr/image\_bmp.bmp\ OK$

The USB camera used supports both YUYV and MJPEG. The collected pictures in the two formats are saved in the /usr folder and can be displayed in the picture browser.

A complete digital image processing system requires an image display system in addition to the image collection system. Add a display interface developed by Qt on Linux to display the collected images.

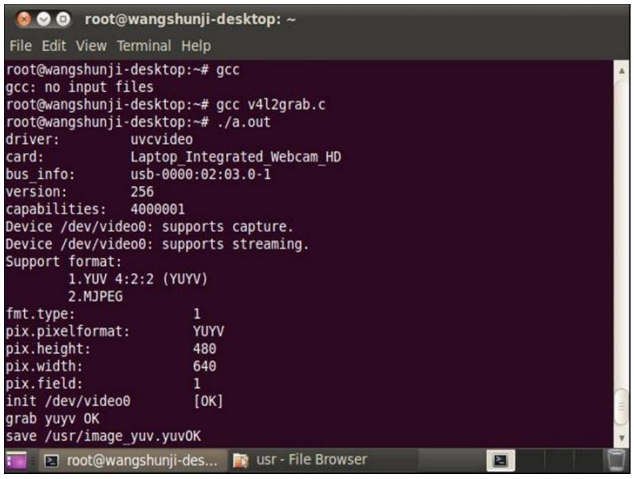

Figure 2: The program obtains the picture successfully.

9 Vector transformation of images

Using a vector drawing computer as input, before drawing, the target image needs to be converted into a vector diagram suitable for the execution of the drawing computer. As shown in Figure 3, the process includes grayscale conversion, binarization, isolated pixel removal, edge refinement [23-24], position restriction, continuous curve detection, synthesis, and other actions.

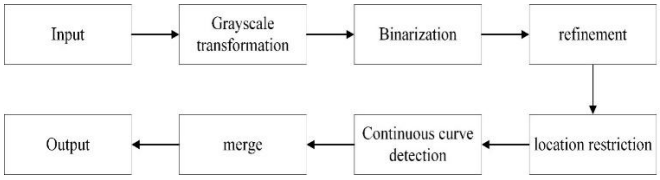

Figure 3: The vector transformation process of the image.

The system uses an image-to-vector procedure to extract vector features from rasterized student outputs for comparison with the standard, ensuring consistent evaluation despite the vector-based nature of AutoCAD drawings, which standardizes various input formats like scanned or non-DXF submissions in Equation (20).

For processing convenience, first, convert the 3-channel color image collected by the camera into a single-channel grayscale image.

$$f = f_R * 0.299 + f_G * 0.587 + f_B * 0.114 \quad (20)$$

Heref_R,f_G,f_B respectively represent a 3-component image in the RGB space, and f represents a transformed grayscale image.

An adaptive threshold technique was used to transform the acquired grayscale image into a binary image [25–26]. Establish the binarization threshold as T ($a \le T \le b$) and ascertain the image's gray value range $[a, b]$ in Equation (21).

$$f_T(x,y) = \begin{cases} 1, f(x,y) \geq T \\ 0, f(x,y) < T \end{cases} \quad (21)$$

The plotter uses it to verify the accuracy of the vector transformation by creating a physical reference by converting standard images to vector paths. The following assures that student drawings are appropriately interpreted by the system's scoring engine, which is based on picture similarity and DXF matching. As a result, both digital and tangible elements support evaluation accuracy and consistency.

Among them, f_T represents the transformed binary image. An example of the transformed effect is shown in Figure 4.

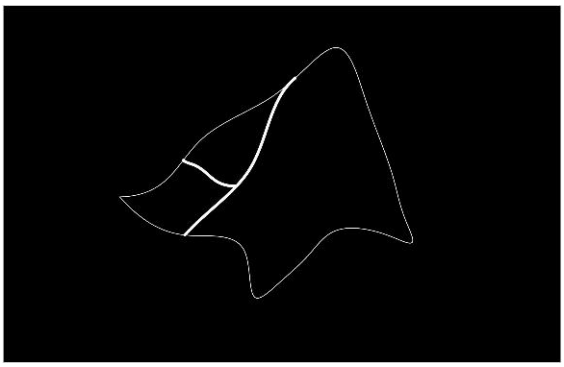

Figure 4: Example of a binarized image.

Through skeleton extraction, the image edge curve with a single pixel width is obtained as shown in Figure 5.

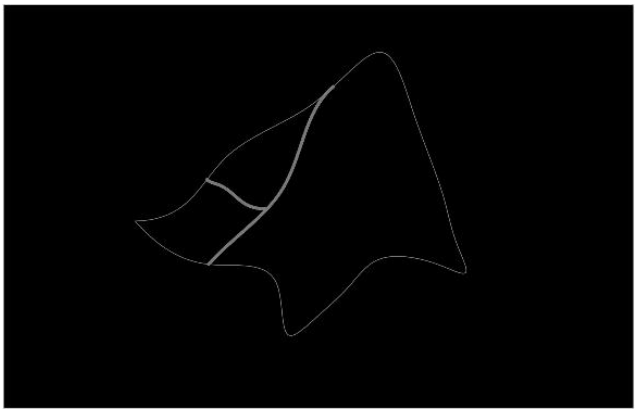

Figure 5: Refinement of the image.

A single-pixel-width edge was consistently formed by the refinement process in Figure 5. For the drawn image to be the center of the canvas, the image must be snapped in position, leaving only the valid portion of the image. The method in this paper first obtains the contour of the effective image through the edge detection algorithm, determines the four outermost pixel points, and then cuts the rectangle determined by the four points to obtain the required image and its coordinate information.

As shown in Figure 6, using different thicknesses to represent different vector curves, the image consists of 4 curves in total.

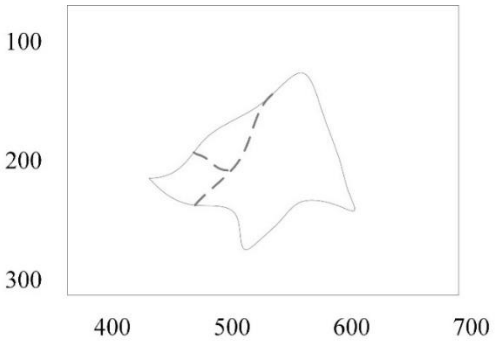

Figure 6: Initial vector curve.

To further advance the drawing effectiveness of the drawing computer and reduce the number of actions of the drawing computer to raise and drop the pen, the divided vector curves are merged, and the adjacent non-closed vector curves are converted into closed curves. As shown in Figure 7, after merging and optimization, the vector curves in the figure are reduced from 4 to 3.

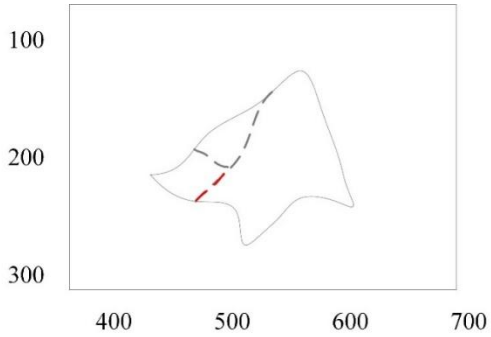

Figure 7: Merged and optimized vector curves.

Vector curves were successfully decreased from 4 to 3 by the merging stage without sacrificing structural integrity in Figure 7 enhancing drawing efficiency. After the above series of image processing operations, the target image to be drawn can be converted into a vector curve recognizable by the drawing computer, and the drawing operation can be performed after being downloaded to the computer actuator.

Therefore, image entropy can be selected as a characterization feature of Chinese paintings, calligraphy images, and man-made images [27-28]. Equation (22) uses the image entropy$p(z_i)(i = 0,1,2,\cdots,L-1)$as a random variable that represents grayscale, where L is the number of identifiable grayscales and the related histogram.

$$e = -\sum_{i=0}^{L-1} p(z_i)\, log_2\, p\,(z_i) \quad (22)$$

From the nature of entropy, the average uncertainty of the equal probability distribution source is the largest, and the uncertainty of the random variable distribution is the largest at this time. The images of Chinese painting and calligraphy are obtained from nature, and artificial images are produced by people's subjective thoughts, so the images of Chinese painting and calligraphy are more complicated than artificial images.

The image's edge, with grayscale variation, boundary, and direction, contains the most image information. Systematic measure measures regional difference, maximal when all levels are equal [29]. The system employs DXF parsing and vector manipulation to address edge scenarios, compensate for scaled or rotated drawings, reduce partial occlusions, and validate components across layers before scoring, thereby preserving grading accuracy and enhancing robustness, while addressing incorrect layer utilization. The appropriate histogram is making$p(z_i)(i = 0,1,2,\cdots,L-1)$, where L is the number of distinct gray levels, and Equation (23) defines the consistency$U$.

$$U = \sum_{i=0}^{L-1} p_2(z_i) \quad (23)$$

From the perspective of the generation mechanism of Chinese paintings, calligraphy images, and artificial images, Chinese paintings, and calligraphy images have local obvious recognition and other local features [30]. Therefore, consistency can be a feature that distinguishes these two images.

The second-order moment (homogeneous variance$\sigma^2(z) = \mu_2(z)$) is another important feature of the identification feature. It represents the measure of gray-level contrast and can establish a descriptor about smoothness, which is expressed by Equation (24).

$$R = 1 - \frac{1}{1+\sigma^2(z)} \quad (24)$$

A region's relative brightness smoothness is measured by its cleanliness. $R = 0$: In the area with constant brightness; $R = 1$ in the area where the gray level value deviates significantly.

10 Compile and make runtime library files

In the directory f where the project is located, use the command qmake-Project to obtain the project file lab2 to generate qtcamera.pro. Then use the qmake command to generate the makefile file, and use make to compile the executable file.

The execution of the Qt software depends on the executable library, which is created and mounted to the reference directory. Go to the directory where the installation files were extracted and enter the following command.

The "Compile and Make Runtime Library Files" part supports the image capture component for image-to-vector transformation, creating reference vector diagrams and verifying robotic drawing reproduction. To ensure end-to-end integrity of the suggested evaluation workflow, supporting visual comparison and physical drawing validation, even though not directly related to CAD scoring. Algorithm 1 displays the command to compile the executable file.

Algorithm 1: Library Files to installation and extracted command

$dd\ if = /dev/zero\ of = qt\_lib\_ext4.img\ bs = 1M\ count = 80$

$mkfs.ext4 - F\ qt\_lib\_ext4.img$

$chmodgo + w\ qt\_lib\_ext4.img$

$mount\ qt\_lib\_ext4.img - o\ loop/mnt$

$cp - rf/usr/local/Trolltech/Qt - 4.7.3/*/ mntchmod\ go - w\ qt\_lib\_ext4.$

img

$umount/mnt$

Therefore, the library files under the /usr/local/troltech/Qt-4.7.3/ folder are all included in the newly made 80M image file. The library is ready.

First, the AutoCAD exam questions are classified according to the knowledge points of the exam. The important functions and knowledge points of AutoCAD are drawing and editing of graphics, dimensions and dimensions, text styles and annotations, setting of environment variables, query, view scale, block, pattern filling, etc. [14]. Each exam question sets a scoring parameter table according to the knowledge points.

The image processing technique is a simulation algorithm that mimics the solid annealing process in real life. This process involves heating and cooling a solid, causing disorder and increasing internal energy [16]. The particles are then sorted slowly, reaching equilibrium at every temperature. The image processing method consists of two stages: drawing processing and recognition. The specific steps include achieving the ground state at room temperature, minimizing internal energy, and achieving the equilibrium state at every temperature.

1) Each rendering packet is sent at a specific time interval, and the source node gets ACK or NAK feedback information to create a feedback matrix T that keeps the update up to current. The origin node processes N rendering packets for K receiving nodes.
2) After the resource node has processed N packets, it enters the retransmission phase with time. All missing packets make up the largest coefficient $D = \{X_1, X_2, X_3, \cdots, X_n\}$ in the set $G = \{g_{i1}, g_{i2}, g_{i3}, \cdots, g_{in}\}(1 \le i \le M_{max}())$ coefficient vector M_{max} (chosen randomly from a limited domain) to recommend all missing plotting packets.F_q generates M_{max} recommendation packages. The maximum number of lost packets at all nodes of M_{max} is Equation (25).

$$M \underset{i\in\{1,2,\cdots,K\}}{max}\left\{\sum_{j=1}^{K} T(i,j)\right\}_{max} \quad (25)$$

3)After resending the recommended drawing package, each receiving node approximates and shows the arrangement of its own recommendation vector matrix G. M_{max} If $r_i \neq N$, the node means that G does not reach the complete permutation, then the node needs to notify the source node and resend some recommended packets, and G can be a complete permutation. Here by indicating the required recommendation grouping, the specific situation in Equation (26)

$$N_i = \begin{cases} N - r_i, r_i \le N \\ 0, r_i \ge N \end{cases} \quad (26)$$

in the formula$i = 1,2,\cdots,K$.

In the drawing resend phase, if the receiving node receives the recommended drawing packet, it is 0. When a node loses two recommended packages R_i M_{max} N_i $R_i$then$N_i =$ 2。

4) The source node updates based on the feedback value of each receiving node, and generates the recommended group key algorithm in the new retransmission stage.N_i $M_{\max}$ M_{max}(4)。

5) 3) and 4) are repeated until all receiving node vector matrices are equal to N. That is, M_{max}, with no lost packets, the receiving node can decode the original drawing packets using Gaussian elimination.

It can be seen that the differences between the ERA and AutoCAD computer drafting methods presented here are mainly shown in the following points.

1) Image processing methods have low complexity in combining lost packets. The AutoCAD computer drawing method needs to update the feedback matrix to determine the different types of packets, and the image processing method not only combines all lost packets for retransmission but also the number of recommended packets is determined by Mmax.

2) The image processing method is not affected by the distribution of lost packets, and the number of recommended packets is determined mainly by the receiving node with the most lost packets. Algorithm 2 shows the pseudocode of the main module.

Algorithm 2 Pseudocode of the main module

```
function main():
Input
 image = getImageInput()
dxf = getDXFInput()
 Preprocessing
gray = toGrayscale(image)
   binary = binarize(gray)
   edges = refineEdges(binary)
vector_img = extractVectors(edges)
 DXF Feature Extraction
student_feats = parseDXF(dxf)
ref_feats = loadReference ()
 Scoring
hist_score = histogramSimilarity (vector_img, ref_feats)
dist_score = sum(manhattanDist(student_feats[i], ref_feats[i]) for i in range(len(ref_feats)))
comp_score = completeness (student_feats, ref_feats)
 Final Score
final_score = 0.5 * hist_score + 0.3 * (1 - normalize(dist_score)) + 0.2 * comp_score
print("Score:", final_score)
```

```
Retransmission & Drawing (Optional)

  packets = feedbackRetransmit(preparePackets(vector_img))

  if final_score>= threshold:

drawRobot(pathPlan(packets))
```

11 Examples and results analysis

In the specific operation of Auto CAD computer drawing pictures, by comparing the answer pictures of the two students with the correct answer pictures, this operation can also test the rationality of the computer program system. The graph is divided into three different types of CAD drawings, the graphs of the same size as the standard picture are cut out, a folder is created to save them together, and then the similarity calculation method is used to calculate the corresponding answer. The import system of the A and B pictures given by the two students is shown in Figures 8 and 9 below.

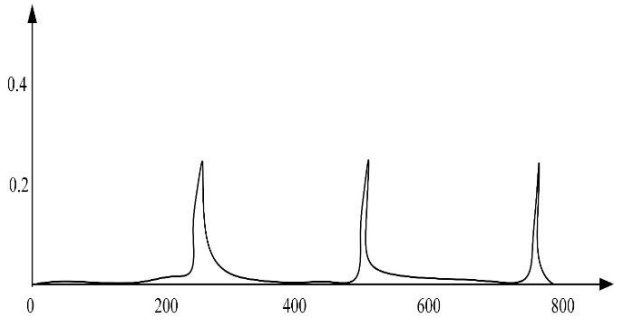

Figure 8: Calculation program for reading A students' scores (92).

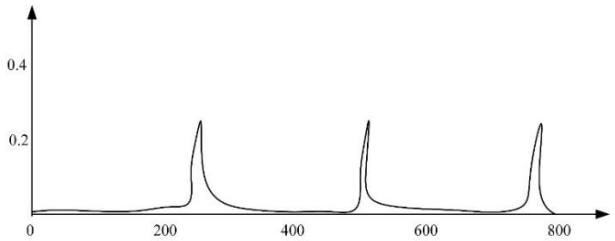

Figure 9: Calculation program for reading B students' scores (80).

Histogram-based comparison methods were used to calculate the similarity scores between the student drawings and the reference. Early instances (Students A and B) are depicted in Figures 8 and 9, which closely match grades assigned by humans.

In the input drawing of student, A, the student has completed the axis, walls, doors and windows, as well as some dimension display, the configuration of stairs and furniture is lacking, and the score of the project test paper is 92. Teachers who graded the papers by hand achieved 92 grades. The input B student diagram completes the display of the axis, doors and windows, part of the wall, and part of the size. The placement of furniture, stairs, and a part of the wall was incomplete, and the score for the program volume was 80. Teachers who manually graded the papers achieved 80 grades. According to the output grades of students A and B, the program calculation results based on the similarity principle are consistent with the integer part of the manually collected results, and the decimal point can be rounded off.

Image similarity and CAD content evaluation are included in the scoring. First, histogram-based similarity is used to compare answer photos to standard images. After that, parsed DXF files are used to evaluate CAD-specific aspects, such as axes, walls, doors, and dimensions. Student A and B's scores (92 and 80) match the hand-assessed results, indicating both visual accuracy and content completeness, which could be explained by the blended technique.

Using the above design scheme, a suspended drawing computer drawing examination system based on a servo motor drive is developed. The main parameters are shown in Table 3.

Table 3: The table of drawing computer parameters

qualit y(kg)	white board height (m)	Hangi ng point spaci ng(m)	Suppl y volta ge(V)	maxim um torque(kg/cm)	Rotatin g speed(ra d/min)
0.335	0.86	0.45	11.1	2.22	300

The servo motor-powered drawing machine physically reproduces digital drawings to verify the accuracy of the system's vector interpretation. The machine provides real execution for verifying vector outputs and evaluating picture processing integrity, ensuring the practical robustness of the suggested AutoCAD evaluation system.

Vectorizer outputs maintained an average speed of 1.75 cm/s and a drawing accuracy of better than 0.1 cm, according to quantitative validation using the drawing robot (Table 3). That suggests the vector conversion pipeline had little distortion. However, when the result is weak contrast edges or overlapping stroke regions during binarization, the method introduces small alignment errors that could impact snapping accuracy or curve continuity. Usually, post-processing techniques like coordinate anchoring and contour-based cropping help to reduce these inaccuracies. As demonstrated by student score comparisons (e.g., students A and B matched human-evaluated scores), the vectorization accuracy generally closely matches manual grading outputs, indicating that

the vector transformation procedure is both mathematically robust and pedagogically reliable for AutoCAD examination assessment.

To facilitate the drawing computer to adjust the drawing position to adapt to different types of whiteboards, an easy-to-operate GUI user interface is designed, which can easily perform target image input, motor position adjustment, whiteboard parameter setting, drawing start and stop control, etc. To validate the strength of the adopted design and the proposed method, a drawing experiment was carried out using the developed drawing computer drawing examination system. After determining the Base and whiteboard height information, perform moment analysis on each force point on the whiteboard, and the results are shown in Figure 10. Among them, Motor Load represents the moment received. It can be seen that the torque is too large only in the area of y=0, and the other areas meet the requirement that the load torque is less than 30% of the maximum torque.

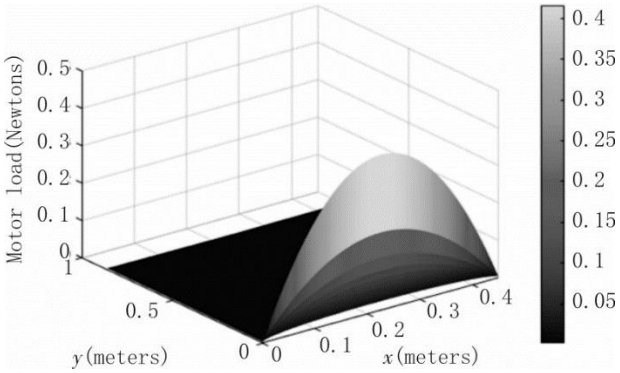

Figure 10: Moment analysis of each point on the whiteboard.

The dead zone positions of the two suspension points are removed, and the positions are limited according to the principle that the load moment is less than 30% of the maximum moment, and the results shown in Figure 11 are obtained.

It can be seen that the motion position does not include the upper left and upper right fan-shaped areas, this is because the two hanging points are positions that the drawing computer cannot reach. In addition, to prevent the motor torque from being too large, the moving area of the drawing computer is limited (the rectangular box area in Figure. 11). To verify the drawing speed and accuracy of the drawing computer, the moving distances of 20 cm, 10 cm, and 5 cm were set respectively, and the average value was obtained after 10 experiments in each group. The outcomes are illustrated in Table 4.

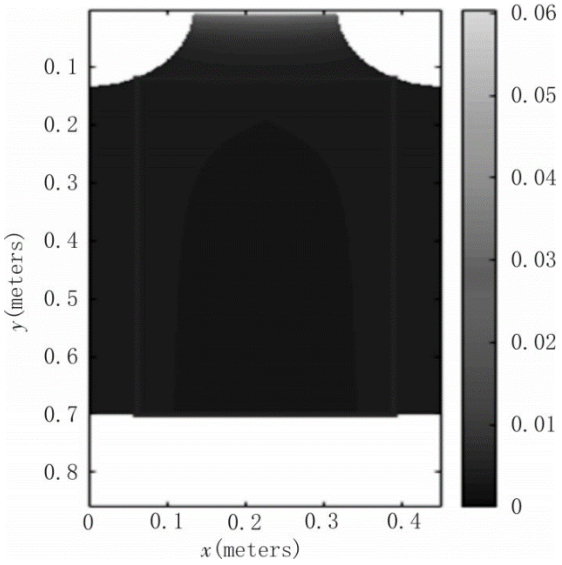

Figure 11: Limiting the movement position of the drawing computer.

Table 4: The experimental results of the drawing speed and accuracy test of the drawing computer.

set distance(cm)	Measured distance(cm)	required time(s)	actual speed(cm/s)	(cm)
20	19.9	11.38	1.749	0.1
10	9.9	5.71	1.733	0.1
5	5.0	2.81	1.780	0.0

From the results in Table 3, it can be seen that the average drawing speed of the computer is 1.75 cm/s, the drawing accuracy is better than 0.1 cm, and the drawing speed and accuracy meet the design requirements. To verify the drawing effect of the drawing computer, several pictures were randomly selected for drawing, and the drawing results are demonstrated in Figure 12.

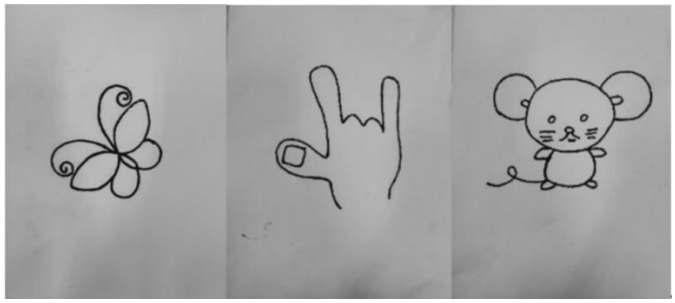

Figure 12: Image rendering example

The proposed AutoCAD assessment system integrates CAD-specific content analysis with histogram-based image similarity for objective, consistent scoring. AutoCAD uses a servo motor-driven drawing machine for physical verification, ensuring higher accuracy, less subjectivity, and practical dependability. The system

surpasses conventional approaches in automation, accuracy, and adaptability for CAD-based examination and assessment activities.

12 Conclusions

For the calculation criteria of the similarity of the pictures, using MATLAB to calculate the picture, the system of drawing the similarity of the pictures, using the students to draw pictures and compare the correct answers, using three different types of pictures and the money-making answers to compare and calculate, calculate and export the correct answer. Realize the function of only scoring by computer. It improves work efficiency and saves manpower and material resources for manual scoring. The development and application market of computer-only scoring systems is ideal. However, a small sample size is a disadvantage. To ensure statistical robustness and show the generalizability of the system's evaluation accuracy, future research will incorporate a broader display of similarity scores across a varied collection of student submissions. Method also features a graphical user interface for user convenience. Complex overlapping designs and problems with contrast could pose problems for the system. Future research could include AI for adaptive scoring refinement, assist 3D CAD review, and improve edge recognition. To demonstrate the method's statistical robustness and generalizability, future research will need to conduct additional examination using a more extensive and varied dataset. A major focus of future research will be thorough statistical validation using larger datasets. The system's analytical depth and evaluation precision will be improved in subsequent work by incorporating quantitative tracking mechanisms during the vector transformation process. The result will allow the calculation of vectorization errors and the identification count of geometric shapes. Large-scale quantitative validation will be incorporated into future research. Future research will take into account more extensive statistical comparisons for a thorough assessment. To enhance item detection and analysis accuracy, future studies will use CNNs trained on annotated CAD datasets to improve drawing structure recognition.

References

[1] Ibarrola F, Lawton T, and Grace K (2023). A collaborative, interactive, and context-aware drawing agent for co-creative design. *IEEE Transactions on Visualization and Computer Graphics*, 30(8), 5525–5537. https://doi.org/10.1109/TVCG.2023.3293853

[2] Fraile-Fernández FJ, Martínez-García R, and Castejón-Limas M (2021). Constructionist learning tool for acquiring skills in understanding standardized engineering drawings of mechanical assemblies in mobile devices. *Sustainability*, 13(6), 3305. https://doi.org/10.3390/su13063305

[3] Quiminsao CMD and Sumalinog JA (2023). Factors affecting the students' achievement and attitude in learning AutoCAD. *Australian Journal of Engineering and Innovative Technology*, 5(3), 130–140. http://dx.doi.org/10.34104/ajeit.023.01300140

[4] Türkyılmaz T (2023). Visual Basic drawing codes from 2D AutoCAD drawings and machine parts applications. *Journal of Innovative Engineering Applications*, 13(2), Article 4. http://dx.doi.org/10.7176/JIEA/13-2-04

[5] de Almeida JS and Baratto NS (2022). Evaluation of screencasts settings applied to CAD online teaching. In: *Más allá de las líneas. La gráfica y sus usos: XIX Congreso Internacional de Expresión Gráfica Arquitectónica*, pp. 639–642. Universidad Politécnica de Cartagena. http://dx.doi.org/10.31428/10317/11414

[6] Li X, Wang X, Li J, Zhang M, Al Ansari MS, and Goyal B (2023). Development of NC program simulation software based on AutoCAD. *Computer-Aided Design and Applications*, Special Issue, S3, 72–83. http://dx.doi.org/10.14733/cadaps.2023.S3.72-83

[7] Gutiérrez de Ravé S, Gutiérrez de Ravé E, and Jiménez-Hornero FJ (2025). Enhancing efficiency and creativity in mechanical drafting: A comparative study of general-purpose CAD versus specialized toolsets. *Applied System Innovation*, 8(3), 74. https://doi.org/10.3390/asi8030074

[8] Eltaief A, Ben Amor S, Louhichi B, Alrasheedi NH, and Seibi A (2024). Automated assessment tool for 3D computer-aided design models. *Applied Sciences*, 14(11), 4578. https://doi.org/10.3390/app14114578

[9] Zhang N, Li F, and Zhang E (2023). The machine vision dial automatic drawing system—Based on CAXA secondary development. *Applied Sciences*, 13(13), 7365. https://doi.org/10.3390/app13137365

[10] Fakhry M, Kamel I, and Abdelaal A (2021). CAD using preference compared to hand drafting in architectural working drawings coursework. *Ain Shams Engineering Journal*, 12(3), 3331–3338. https://doi.org/10.1016/j.asej.2021.01.016

[11] Hsu HH, Wu CF, Cho WJ, and Wang SB (2021). Applying computer graphic design software in a computer-assisted instruction teaching model of makeup design. *Symmetry*, 13(4), 654. https://doi.org/10.3390/sym13040654

[12] Zhang J (2025). Attention mechanism-enhanced model for automated simple brush stroke painting. *Informatica*, 49(20). https://doi.org/10.31449/inf.v49i20.7688

[13] Cheng J, Yang L, and Tong S (2024). Recognition and analysis of painting styles with the help of computer vision techniques. *Informatica*, 48(21). https://doi.org/10.31449/inf.v48i21.6891

[14] Zhao YQ (2017). Transcending images and forms: The theory of expressive aesthetic value of traditional

Chinese freehand painting. *Journal of Aesthetic Education*, 10(8), 3023–3034.

[15] Lu G (2018). An analysis of the application of traditional painting and calligraphy elements in the design of theme hotels. *Journal of Heihe University*, 32(4), 329–335.

[16] Jian M, Dong J, Gong M, Yu H, Nie L, and Yin Y (2020). Learning the traditional art of Chinese calligraphy via three-dimensional reconstruction and assessment. *IEEE Transactions on Multimedia*, 22(4), 970–979. https://doi.org/10.1109/TMM.2019.2931390

[17] Wang G, Zhao S, Liu S, and Siyu L (2017). Micro-arrayed stretch drawing process of nanocrystalline Ni-Co foils with soft-male-die. *Journal of Materials Processing Technology*, 78(4), 110–120.

[18] Lee IK, Lee SY, Kim DH, Lee JW, and Lee SK (2018). Wire drawing process design for fine rhodium wire. *Transactions of Materials Processing*, 15(8), 370–374.

[19] Wang Y (2018). Digital subsistence of Chinese calligraphy fonts. *Packaging Engineering*, 215(1), 806–820.

[20] Yang Q (2018). Technical operation analysis of Photoshop in Premiere header image processing. *China Computer & Communication*, 93(3), 1–8.

[21] Nakagawa M, Sutou K, and Hayakawa T (2020). Reproduction of additive-type fluorescence moiré fringes by image drawing software and study of accuracy of fluorescence imprint alignment. *Japanese Journal of Applied Physics*, 5(5), 445–452. https://doi.org/10.35848/1347-4065/ab5cbe

[22] Lin J and Chen H (2019). Application of image processing technology in graphic design. *Modern Electronics Technique*, 73(7), 40–55.

[23] Cao G (2018). The history and aesthetic features of Chinese literati painting. *Journal of Tianjin Academy of Fine Arts*, 29(7), 143–148.

[24] Cheng H, Huijie L, Luo R (2019). Research on geometric characteristics of asphalt mixture aggregate based on image processing. *Journal of Wuhan University of Technology (Transportation Science & Engineering)*, 21(5), 773–791.

[25] Yin Y and Antonio J (2020). Application of 3D laser scanning technology for image data processing in the protection of ancient building sites through deep learning. *Image and Vision Computing*, 102(5), 173–196. https://doi.org/10.1016/j.imavis.2020.103982

[26] Yang S, Zhang X, and Wang F (2017). Application of map GIS image analysis system in making design drawing of regional gravity points. *Geological Survey of China*, 32(4), 329–335.

[27] Wang C and Han D (2017). Research on the construction of graphic image cooperative processing system based on HTML5 technology. *Boletin Tecnico / Technical Bulletin*, 55(15), 375–384.

[28] Timoftei S (2018). Industrial robot in fine art: Can an industrial robot draw a binary image? *IOP Conference Series: Materials Science and Engineering*, 78(4), 110–120. https://doi.org/10.1088/1757-899X/399/1/012019

[29] Feng M, Ying L, Sun G, Dong Y, Zhang F, and Liu Y (2018). Adaptive processing of dimensioning tire patterns in engineering drawings. *Chinese Journal of Automotive Engineering*, 15(8), 370–374.

[30] Wang G, Liu S, Liu Q, Zhao S, Zhao X, and Li Y (2017). Micro-arrayed stretch drawing process of nanocrystalline Ni-Co foils with soft-male-die. *Journal of Materials Processing Technology*, 240(4), 806–820. https://doi.org/10.1016/j.jmatprotec.2016.10.038